JOURNAL OF OPTOELECTRONICS AND ADVANCED MATERIALS Vol. 9, No. 10, October 2007, p. 3210 - 3214

Effect of phase transition on the optical properties of In_xSe_{1-x} thin films

FALAH I MUSTAFA, AKSHAY KUMAR, N. GOYA, S.K. TRIPATHI*
Department of Physics, Centre of Advanced Study in Physics, Panjab University, Chandigarh-160 014, India

Thin films of chemical composition In_xSe_{1-x} (x = 0.50 and 0.60 at %) are prepared by thermal evaporation technique. The optical properties of these thin films are determined by a method, based only on the transmission spectra at normal incidence, measured over the 400-2000 nm spectral range. This useful optical method takes into consideration the non-uniform thickness of thermally evaporated thin films. The dispersion of refractive index is discussed in terms of the single-oscillator Wemple and DiDomenico model. The optical absorption edge is described using the non-direct transition model proposed by Tauc and the optical band gap (E_g^{opt}) is calculated from the absorption coefficient (α) values by Tauc's extrapolation procedure. It has been found that the value of refractive index (n), real dielectric constant (ε') and oscillator strength (E_d) increase while extinction coefficient (k), imaginary dielectric constant (ε''), average energy gap (E_0) and E_g^{opt} decrease as the In concentration increases. These results have been explained on the basis of phase transition which is taking place in InSe thin films.

(Received July 3, 2007; accepted October 1, 2007)

Keywords: In-Se thin films, Chalcogenide glasses, Optical properties, Band gap

1. Introduction

Interest in optical properties of chalcogenide glasses has been recently increased as they are very promising materials for use in optoelectronic applications [1]. These glasses are very interesting materials for infrared optics. They have a large range of transparency (~ 0.6 to 30 μm) and good mechanical and chemical properties, such as hardness, adhesion, low internal stress and water resistance. The low characteristic vibrational frequencies of chalcogenide bonds allow them to transmit far out into the infrared [2]. These glasses show a variety of photo-stimulated phenomena when exposed to light or other radiations [3-7]. When these glasses are irradiated with high energy particles or light, bond breaking and bond rearrangement can take place, which result in the change in local structure of the glassy materials. These include subtle effects such as shifts in the absorption edge (photo-bleaching and photo-darkening), and more substantial atomic and molecular reconfiguration such as photo-induced refractive index changes and photo-doping effects [8,9]. In general, these phenomena are associated with the changes in the optical constants [10,11] and absorption edge shift [12].

InSe is a semi conducting layered compound that has been a subject of several investigations in recent years. The layer structure is characterized by the covalent bond which is restricted in two dimensions in the plane of the layer and with Van der Waals forces in the third dimensions. These films have typical characteristics of semiconductor layers such as, (i) the low density of dangling bonds on the surface because of the almost complete chemical bonds within the layer [13], (ii) intercalation [14] and (iii) the mechanical weakness due to the weak Van der Waals force between the layers. InSe is a candidate material to form the heterojunction with a very low density of interface states. The phase change takes place in this material when the concentration of In changes above a certain proportion. Data storage devices utilizing the properties of phase change materials are expected to play an important role in multimedia applications in the near future [15,16]. One of the key problem in phase change material applications is the density of data storage, which is determined mainly by the bit size. Therefore, the authors have decided to study the effect of In concentration on optical properties of InSe semi conducting material. The experimental details and the characteristics of the samples are described in Section 2. The results have been presented and discussed in section 3. The last section deals with the conclusions of the present work.

2. Experimental procedure

Glassy alloys of In_xSe_{1-x} (x = 0.50 and 0.60 at %) are prepared by melt quenching technique as described elsewhere [17]. Thin films of the alloys are prepared by vacuum evaporation technique on well-degassed Corning 7059 glass substrates at room temperature and base pressure of ~ 2×10^{-5} mbar using a Molybdenum boat. The deposition rate is very slow so, that the composition of thin film is very close to the composition of the starting bulk material. X-ray diffraction patterns have been taken of both the samples. The XRD of substrate with and without In_xSe_{1-x} thin films have been measured. No prominent peak has been observed in In concentration at 0.50 at %, however, at an In concentration ~ 0.60 at %,

sharp peak has been found which indicates that the phase transition takes place in InSe system.

The normal incidence transmission spectra of the substrate with and without In_xSe_{1-x} (x = 0.50 and 0.60 at %) thin films have been measured by a double beam UV/VIS/NIR computer controlled spectrophotometer [Hitachi-330], in the transmission range 400-2000 nm. The spectrophotometer is set with a suitable slit width of 2 nm in the measured spectral range. It is, therefore, unnecessary to make slit-width corrections, since this slit-width value is much smaller than the different line-widths. The line-width is simply taken to be the width between the two interference extremes immediately adjacent to the one under consideration. The area of illumination over which a single transmission spectrum is obtained is 1mm × 10mm. All the optical constants measurements reported in this paper are performed at room temperature (300 K).

3. Theory

The model behind Swanepoel's method [18,19] assumes that the sample is a thin film of uniform thickness deposited on a transparent substrate having a refractive index '*s*'. The system is surrounded by air, whose refractive index is $n_0 = 1$. The film has a complex refractive index $n^* = n - i\,k$, where n is the refractive index and k the extinction coefficient, which is related to the absorption coefficient (α) through the relation, $k = \alpha\,\lambda / 4\,\pi$. The optical constants are obtained by using only the transmission spectrum. According to this method, which is based on the approach of Manifacier *et al*. [20], the refractive index in the region where $\alpha \approx 0$ is calculated by the following equation:

$$n = \sqrt{N + \sqrt{N^2 - s^2}} \tag{1}$$

where

$$N = 2s\frac{T_{\max} - T_{\min}}{T_{\max}T_{\min}} + \frac{s^2 + 1}{2} \tag{2}$$

T_{max} and T_{min} are the values of the envelope curves $T_{max}(\lambda)$ and $T_{min}(\lambda)$ at the wavelengths in which either the upper or lower envelope and the experimental transmission spectrum are tangent respectively, as shown in Fig. 2. The accuracy to which λ can be measured is ±1 nm. The maximum absolute accuracy of T_{max} and T_{min} is ±0.001. The values of n are calculated using Eq. (1) at the same wavelength as T_{max}, T_{min} and *s*.

If n_1 and n_2 are the refractive indices at two adjacent tangent points at λ_1 and λ_2, then according to the basic equation for interference fringes

$$2nt = m\lambda \tag{3}$$

where '*t*' is the film thickness and 'm' is an order number. The thickness is given by

$$t = \frac{\lambda_1\,\lambda_2}{2(\lambda_1 n_2 - \lambda_2 n_1)} \tag{4}$$

It should be noted that owing to optical absorption the error in 'n' is appreciable and, consequently, the error propagated to 't' through equation 4 is significant [18]. Thus, the values of thickness will be calculated using equation (4) and the estimated average value will be used with the values of 'n' (earlier calculated values using equation 1) to determine the order numbers (m) for the extremes from equation (3). A big increase in accuracy now results in taking the exact integer or half integer values of 'm' for each 'λ'. The value of 'm' is an exact integer where constructive interference occurs, i.e. maxima in transmission curve and half integer where destructive interference occurs, i.e. minima in transmission curve. By using the earlier calculated values of refractive index (using eq. 1), the new values of thicknesses have been calculated (using eq. 3). Using the values of 'm' and the average of these new thickness values, the new values of refractive index has been calculated for each 'λ' as suggested by Swanepoel [18,19].

The extinction coefficient k can be calculated using relation

$$k = \alpha\lambda/(4\pi) = (\lambda/4\pi d)\ln(1/x) \tag{5}$$

The absorption coefficient (α) [19] can be calculated from the relation

$$x = \exp(-\alpha.t) \tag{6}$$

where *x* is absorbance, given by

$$x = \frac{E_M - \sqrt{E_M^2 - (n^2-1)^3(n^2 - s^4)}}{(n-1)^3(n - s^2)} \tag{7}$$

and

$$E_M = \frac{8n^2 s}{T_{\max}} + (n^2 - 1)(n^2 - s^2) \tag{8}$$

The dielectric constant of In_xSe_{1-x} films can be calculated with the help of refractive index (n) and extinction coefficient (k) [21]. Real dielectric constant (ε') can be calculated as given below:

$$\varepsilon' = n^2 - k^2 \tag{9}$$

While the imaginary dielectric constant (ε'') can be calculated as given below:

$$\varepsilon'' = 2nk \tag{10}$$

The absorption coefficient of amorphous semiconductors in the strong-absorption region ($\alpha \geq 10^4$ cm^{-1}), assuming parabolic valence and conduction band edges, is given by [22]

$$\alpha(\hbar\omega) = \frac{B(\hbar\omega - E_g^{opt})^2}{\hbar\omega} \tag{11}$$

where $\hbar\omega$, E_g^{opt} and B, represent photon energy, optical gap and an energy independent constant, respectively. Finally, the optical gap is calculated from the intersection of the plot $(\alpha\hbar\omega)^{1/2}$ vs. $\hbar\omega$ with the abscissa axis. The refractive index dispersion $n(\lambda)$ can be fitted by the Wemple-DiDomenico relation [23,24].

4. Results and discussion

Fig. 1 (a) and (b) show the X-ray diffraction patterns of $In_{50}Se_{50}$ and $In_{60}Se_{40}$ thin films. It is clear from the figures that there is no sharp peak present in $In_{50}Se_{50}$ film. However, a sharp peak has been observed in $In_{60}Se_{40}$ thin film which indicates a transition from amorphous to crystalline takes place. The particle size has been calculated and found to be ~ nm using the Debye-Scherrers formula [25] as given below:

$$\beta = 0.9\,\lambda / D\cos\theta \tag{12}$$

where β is the broadening of diffraction line measured at half its maximum intensity and D is the diameter of crystal particle.

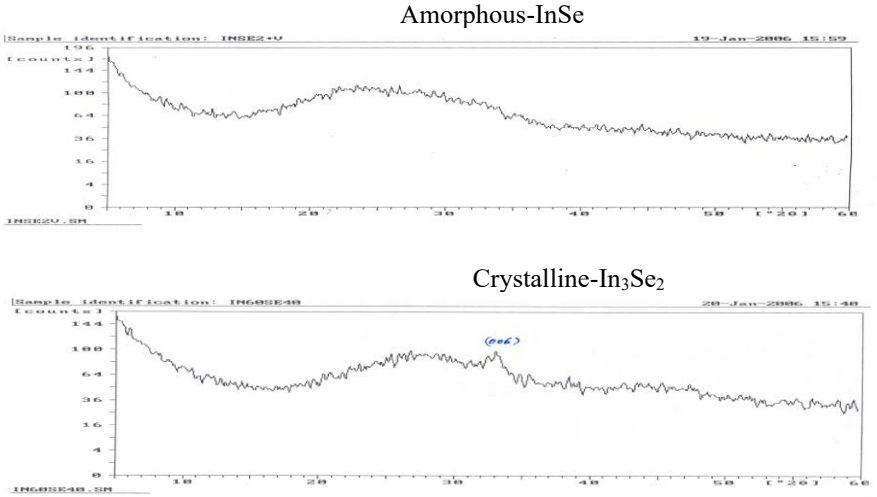

Fig. 1. XRD patterns of In_xSe_{1-x} thin films.

Fig. 2 shows the optical transmission spectra $T(\lambda)$ of a-$In_{0.50}Se_{0.50}$ thin film. The values of n are calculated for both samples using Eq. (1) at different wavelengths corresponding to tangent points (T_{max} and T_{min}). On the other hand, the data on the dispersion of the refractive index, $n(\lambda)$ have been calculated using the single-effective-oscillator model proposed by Wemple and DiDomenico [23,24].

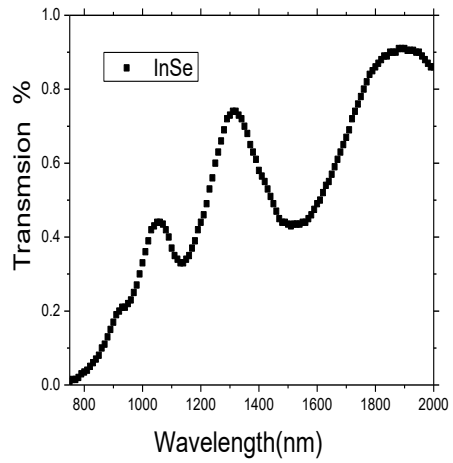

Fig. 2. Transmission spectrum of a-$In_{50}Se_{50}$ thin film.

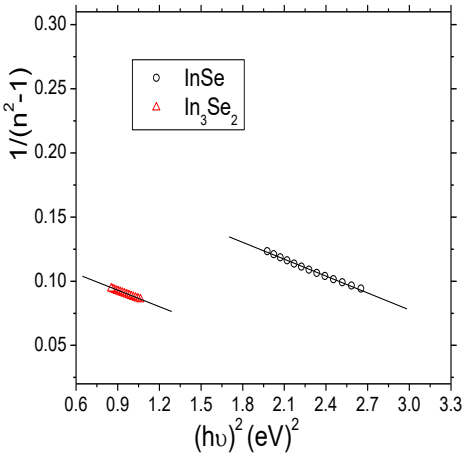

Fig. 3. Plot between $1/(n^2-1)$ and $(\hbar\omega)^2$.

They found that all the data can be described to an excellent approximation by the following relation:

$$n^2(\hbar\omega) = 1 + \frac{E_d E_0}{E_0^2 - (\hbar\omega)^2} \tag{13}$$

where $\hbar\omega$ is the photon energy, E_d is the oscillator strength and E_0 is the energy of the effective dispersion oscillator (typically near the main peak of the loss part of dielectric function ε_2 – spectrum), which is identified by the mean transition energy from the valence band of the lone-pair

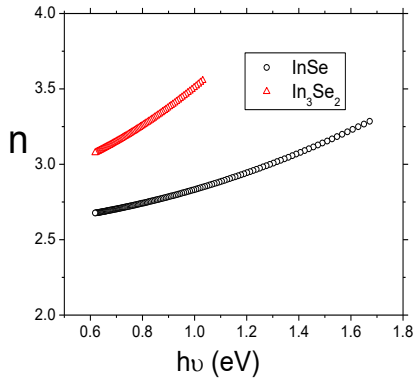

Fig. 4. Variation of experimentally calculated and Wemple-DeDomenico fitted (WDF) values of n with wavelength (λ).

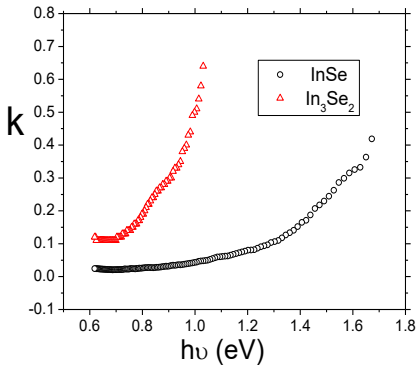

Fig. 5. Variation of extinction coefficient (k) with energy in In_xSe_{1-x} thin films.

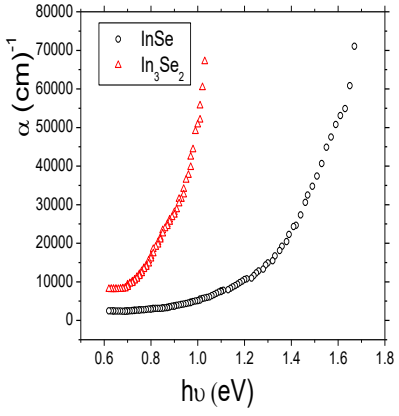

Fig. 6. Variation of absorption coefficient with energy.

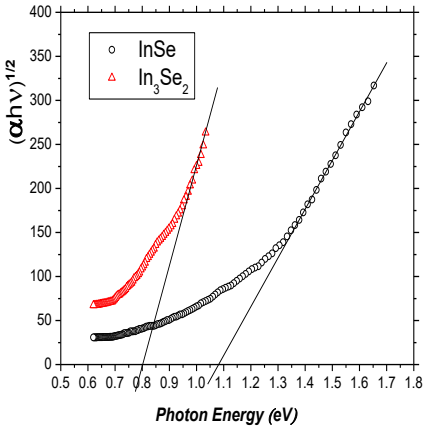

Fig. 7. Plot between $((\hbar\omega)^{1/2}$ and $\hbar\omega$.

Table 1

Material	E_g (eV)	E_o (eV)	E_d (eV)	n (at λ=1300 nm)	k (at λ=1300 nm)
InSe	1.08	2.21	10.53	2.90	0.03
In_3Se_2	0.81	1.79	9.52	4.09	0.34

The refractive-index dispersion from the Wemple-DeDomenico model is shown in Fig. 4 for all samples, together with the refractive indices derived using present characterization method. It is clear from the figure that the value of n increases as the concentration of In increases in InSe system at all wavelengths. Fig. 5 shows the variation of extinction coefficient (k) with different photon energies. It is clear from the figure that the value of k increases with the increase of photon energy and with the increase of In concentration.

The value of absorption coefficient (α) is calculated at different energies and plotted in Fig. 6. The value of α increase at all energies after the In concentration is increased in InSe system. The optical gap (E_g^{opt}) is determined from the intercept on the energy axis of the linear fit of the larger energy data, in a plot of $(\alpha\hbar\omega)^{1/2}$ vs. $\hbar\omega$ (Tauc extrapolation [22]). Fig. 7 shows $(\alpha\hbar\omega)^{1/2}$ vs. $\hbar\omega$ for the calculation of E_g^{opt}. The values of n, E_g^{opt} for both samples are given in Table 1.

It is clear from the above results (see Fig. 1) that the phase transition i.e. from amorphous ($In_{50}Se_{50}$) to crystalline ($In_{60}Se_{40}$) takes place. Due to this phase transition, the density of micro crystallites is high and the percolation threshold has been reached. In case of $In_{50}Se_{50}$ thin films, the densities of the micro crystallites are far smaller and we are below the percolation threshold. Due to the higher density of micro crystallites, the value of refractive index (n) increases (see table 1) in case of $In_{60}Se_{40}$ thin films. A transition from p → n has been

reported in InSe alloy when the concentration of In increases above a certain level [26,27] and this has been attributed to the percolation threshold between these crystallites.

5. Conclusions

The optical properties of In_xSe_{1-x} thin films have been measured and calculated from the transmission spectra by using Swanepoel's method. The experimentally calculated values of refractive index are in good agreement with Wemple Didomenico fitting expression of refractive index. There is a good consistency between the results obtained in the present work and those previously reported by other authors for related alloys. A phase transition from amorphous to crystalline takes place as the concentration is increased from 0.50 to 0.60 at % of In. Increasing the In concentration into the InSe system introduces the excess electronic delocalized states into the InSe binary system. We have analyzed the optical-dispersion data using the Wemple-DeDomenico single-effective-oscillator model. The change in the refractive index after increasing the In concentration into InSe glass, makes this system an attractive candidate as optical recording medium.

Acknowledgements

This work is financially supported by CSIR (Major Research Project) New Delhi.

References

[1] A. M. Andriesh, M. S. Iovu, S. D. Shutov, J. Optoelectron. Adv. Mater. **4,** 631 (2002).
[2] P. J. S. Ewen, C. W. Shinger, A. Zakery, A. Zekak, A.E. Owen, SPIE Infrared Optoelectron. Mater Dev. **1512**, 101 (1991).
[3] A. Ganjoo, N. Yoshida, K. Shimakawa, Recent Res. Dev. Appl. Phys. **2**, 129 (1999).
[4] M.S. Iovu, S.D. Shutov, M. Popescu, J. Non-Cryst. Solids **299**, 924 (2002).
[5] S.K. Tripathi**,** A. Thakur, G. Singh, J. Sharma, V. Sharma, K.P. Singh, G.S.S. Saini and N. Goyal, J. Optoelectron. Adv. Mater. **7**, 2095 (2005).
[6] A. Arsh, M. Klebanov, V. Lyubin, L. Shapiro, A. Feigel, M. Veinger, B. Sfez, Optical Mat. **26**, 301 (2004).
[7] V. Lyubin, M. Klebanov, A. Feigel, B. Sfez, J. Non-Cryst. Solids **459**, 183 (2004).
[8] N. Goyal, A. Zolanvari, S.K. Tripathi, J. Material Science: Materials in Electronics **12**, 523 (2001).
[9] M. Mitkova, M.N. Kozicki, H.C. Kim, T.L. Alford, J. Non-Cryst. Solids **338**, 552 (2004).
[10] L. Tichy, H. Ticha, P. Nagels, R. Callaerts, R. Mertens, M. Vlcek, Materials Letters **39**, 122 (1999).
[11] J.M. Gonzalez-Leal, A. Ledesma, A.M. Bernal-Oliva, R. Prieto-Alcon, E. Marquez, J.A. Angel, J. Carabe, Materials Letters **39**, 232 (1999).
[12] V.M. Lyubin, M. Klebanov, B. Sfez, B. Ashkinadze, Mat. Letts. **58**, 1706 (2004).
[13] S. Gopal, C. Viswanathan, B. Karunagaran, Sa. K. Narayandas, D. Mangalraj and Junsin Yi, Cryst. Res. Technol. **40**, 557 (2005).
[14] B. Fotouhi, O. Gorochov, A. Katty, N. Le Nagard, C. Levy-Clement, D. Schleich, B. Theys H. Tributsch, Scl. Energy Res. Dev. Eur. Community. Ser. D **2**, 78 (1983).
[15] J. W. Toigo, Sci. Am., **282**, 50 (2000).
[16] G.A. Gibson, A. Chaiken, K. Nauka et al, Appl. Phys. Lett. **86**, 051902 (2005).
[17] S.K. Tripathi, Vineet Sharma, Anup Thakur, G.S.S. Saini, N. Goyal, J. Non-Cryst. Solids **351**, 2468 (2005).
[18] R. Swanepoel, J. Phys. E: Sci. Instrum. **17**, 896 (1984).
[19] R. Swanepoel, J. Phys. E **16**, 1214 (1983).
[20] J.C. Manifacier, J. Gasiot, J.P. Fillard, J. Phys. E: Sci. Instrum. **9**, 1002 (1976).
[21] M.M. Wakkad, E.Kh. Shoker, S.H. Mohamed, J. Non-Cryst. Solids **157**, 265 (2000).
[22] J. Tauc, A. Menth, J. Non-Cryst. Solids **8**, 569 (1972).
[23] S. H. Wemple, M. DiDomenico, Phys. Rev. B **3**, 1338 (1971).
[24] S. H. Wemple, Phys. Rev. B **7**, 3767 (1973).
[25] R.B. Kale, S.D. Sartale, B.K. Chougule, C.D. Lokhande, Semicond. Sci. Technol. **19**, 980 (2004).
[26] A. Segura, J.P. Guesdon, J.M. Besson, A. Chevy, J. Appl. Phys. **54**, 867 (1983).
[27] C. De Blasi, G. Micocci, A. Rizzo, Phys. Rev. B **27**, 2429 (1983).

*Corresponding author: surya@pu.ac.in; surya_tr@yahoo.com